Available online at www.sciencedirect.com
SCIENCE DIRECT®
Spectrochimica Acta Part A 61 (2005) 2041–2047
SPECTROCHIMICA ACTA PART A
www.elsevier.com/locate/saa

Study on the interaction of new water-soluble porphyrin with DNA

Jingwan Kang*, Haixia Wu, Xiaoquan Lu, Yongsheng Wang, Lin Zhou

Department of Chemistry, Northwest Normal University, Gansu China, Lanzhou 730070, P.R. China

Received 1 May 2004; accepted 18 August 2004

Abstract

A porphyrin meso-tetrakis{[4-(1-pyridyl)propoxy]phenyl}porphyrin (TPyPP) and its Ni complex (TPyPP(Ni)) have been synthesized and characterized by ^{1}H NMR, UV–vis spectra. The interaction of two porphyrins with calf thymus-DNA (CT-DNA) has been explored by UV–vis, fluorescence and circular dichroic spectroscopy and viscosity measurements. The results suggest that these porphyrins can bind to DNA by the same binding mode. TPyPP outside binds by self-stack with DNA both at low drug load *r* (=[porphyrin]/[DNA]) and high drug load. Though TPyPP(Ni) has center metal nickel, binding mode with DNA has little difference compared with TPyPP, dominating out-binding mode with different direction along DNA. The binding constants of the TPyPP and TPyPP(Ni) to DNA were $4.65 \times 10^5\ M^{-1}$ and $3.2 \times 10^5\ M^{-1}$, respectively. A colored precipitate was found after time in two porphyrin's viscosity measurement. The reasonable interpretation is the porphyrins with alkyl connected N-position of pyridine can strongly interact with the anionic phosphates of DNA and lead to hydrophobic complex.

Keywords: Water-soluble porphyrin; DNA; Out-binding

1. Introduction

Interaction of porphyrins and metalloporphyrins with DNA has a considerable interest due to their medical applications. Their special properties: high optical absorption, relatively high quantum yields of triplet state and fluorescence, or paramagnetism of some metal complexes, provide the use of porphyrin in medicine, as active compounds in radiological [1,2], and magnetic resonance imaging [3,4] of cancer detection and as photosensitizers in photodynamic therapy (PDT) of cancer [5,6]. Porphyrin demonstrates the photodynamic activity against psoriasis atheromatous plaque, viral and bacterial infections including HIV as well [7].

Cationic porphyrins are considered as double functional compounds that strongly bind to DNA and photo dynamically modify the target site of a DNA molecule by a mechanism similar to that of anti-cancer antibiotics such as bleomycin and daunomycin based on the DNA cleavage [8–10]. The interaction of cationic porphyrins with synthetic and natural DNA has been widely studied using visible absorption spectroscopy and circular dichroism (CD) [11–13], fluorescence [14], Raman [15], NMR [15,16], ESR [17], viscometry [18,19], footprinting [20,21], kinetic methods [22] and X-ray crystallography [23].

There are a number of advantages of studying the DNA binding interactions of cationic metalloporphyrins. First, that these molecules bind to nucleic acids in ways similar to"real" anti-tumor drugs, i.e., by intercalative or external binding modes, makes these porphyrins powerful probes of drug-DNA interactions, as well as DNA structure. Second, their high solubility and weak tendency to aggregate in water (except at very high porphyrin concentrations) make them suitable for investigation under a wide variety of solution conditions. Third, by varying the metal center and peripheral substituents, the porphyrin's binding mode to nucleic acid duplexes can be easily "tuned" to be the intercalative or external type. For example, the thin square planar Cu^{II}; Ni^{II} derivatives of meso-tetrakis (*N*-methylpyridinium-4-yl)porphyrin ($H_2P(2)$) are capable of intercalation, since

* Corresponding author. Tel.: +86 931 7972613; fax: +86 931 7971697.
E-mail address: jwkang@nwnu.edu.cn (J. Kang).

1386-1425/$ – see front matter © 2004 Elsevier B.V. All rights reserved.
doi:10.1016/j.saa.2004.08.009

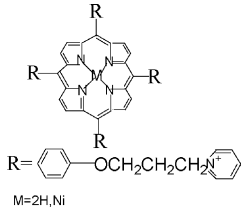

Scheme 1. Structure of porphyrin.

these metalloporphyrins do not ligate H_2O molecules at their vacant axial sites and can be inserted into the pocket between two adjacent, closely spaced (3.4 Å) B-DNA base pairs.

Three major binding modes have been proposed for the binding of cationic porphyrins to DNA: intercalation, outside groove binding and outside binding with self-stacking in which porphyrins are stacked along the DNA helix [12,24–26]. One motivation for these spectroscopic investigations has been to establish empirically reliable criteria for differentiating between the intercalative and outside binding modes of porphyrins with various synthetic and native DNAs. A thorough, initial investigation conducted in Pasternack's laboratory showed [11]: that intercalating porphyrins are characterized by: (i) large red ($\Delta\lambda \geq 15$ nm) and hypochromic ($H \geq 35\%$) shifts of their Soret maxima, (ii) negative (−) induced CD activity in the Soret region, and (iii) high selectivity for GC-rich DNA sequences. In contrast, outside binders displayed: (i) much smaller red shifts ($\Delta\lambda \leq 8$ nm) and little hypochromicity ($H \leq 10\%$), and sometimes hyperchromicity) of their Soret maxima, (ii) positive (+) induced CD bands in the Soret region, and (iii) a distinct preference for AT-rich minor groove segments.

The extensive exploration of cationic porphyrins has been hitherto limited to cationic porphyrins with alkyl connected 4-position of pyridine and its various derivates. In the present study, we synthesized a cationic porphyrins with alkyl connected N-position of pyridine: meso-tetrakis{[4-(1-pyridyl)propoxy]phenyl}porphyrin (TPyPP) and its Ni complex (the structure as shown in Scheme 1). The interaction of the porphyrins with calf thymus-DNA (CT-DNA) was studied on the basis of their spectral changes in the Soret band and induced CD in the visible region as well as fluorescence spectra and viscosity measurement.

We find TPyPP bind DNA by self-stacked outside binding and electrostatic interaction. While TPyPP(Ni) has center nickel which do not ligate H_2O molecules at its vacant axial site but it bind DNA by an outside binding mode and electrostatic interaction.

2. Experimental

2.1. Materials and instruments

All chemicals were analytical grade. Pyrrole was freshly distilled before use. Calf thymus-DNA was purchased from purchased from Sino-American Biotechnology Company (Beijing, China). UV–vis spectra were recorded in solutions on UV-3400 spectrophometer (Hitachi, Japan). Fluorescence spectra were carried out using RF-540 spectrofluorophometer (Hitachi, Japan). CD spectra were recorded on a Jasco-20C spectropolarimeter (Japan). ^{1}H NMR spectra using Brucker AM-400. Meso-tetrakis[4-(3-bromopropoxy)phenyl]porphyrin was obtained by method [27].

2.1.1. Synthesis of meso-tetrakis{[4-(1-pyridyl)-propoxy]phenyl}porphyrin

Meso-tetrakis[4-(3-bromopropoxy)phenyl]porphyrin (50 mg) was dissolved in 50 ml anhydrous chloroform. The solution was heated to refluxing and 1.3 ml pyridine was added. The mixture was refluxed for 48 h, and then removed solvent. The residue was washed by acetone for three times. The yield was 85% ^{1}H NMR (DMSO-d_6): δ 9.33(d,8H, α-py-H) 8.82(s,8H, β-pyrrole) 8.69(t,4H, β-py-H) 8.29(t,8H,r-py-H) 8.17–8.10(m,8H,ph-H) 7.24(d,8H,ph-H) 5.01–4.98(t,8H,Ar-OCH_2-) 4.42(t,8H,-CH_2py) 2.65–2.49(m,8H, $ArOCH_2CH_2$-) −2.94(s,2H,NH)

UV–vis (phosphate buffer pH = 7.0) λ_{max} (nm): 421, 517, 554.4, 590, 646.6.

2.1.2. Synthesis of meso-tetrakis[4-(3-bromopropoxy)-phenyl]porphyrin nickel

Meso-tetrakis[4-(3-bromopropoxy)phenyl]porphyrin (50 mg) was dissolved in 50 ml toluene and heated to reflux. Then (1 g) nickel acetate was added. The mixture was refluxed for 5 h then removed solvent. The residue was washed by water and obtained a purple crystal of porphyrin with yield of 80%.

2.1.3. Synthesis of meso-tetrakis{[4-(1-pyridyl)-propoxy]phenyl}porphyrin nickel

The complex was prepared by a procedure similar to that TPyPP.

^{1}H NMR(DMSO-d_6): δ 9.36(d,8H, α-py-H) 8.77-8.72(m,12H, β-pyrrole, β-py-H) 8.32–8.29(m,8H, r-py-H) 8.13(m,8H,ph-H) 7.92(m,8H,ph-H) 7.34–7.18(m,8H,ph-H) 4.98(t,8H, $ArOCH_2$-) 4.38(t,8H, CH_2py-) 2.64(m,8H, $ArOCH_2CH_2$-).

UV–vis (phosphate buffer pH = 7.0) λ_{max}(nm): 419, 525.6, 648.8.

2.2. Spectral measurements

All experiments, except where specially indicated, were performed at room temperature in a phosphate buffer pH 7.0 consisting of 6.1 mM Na_2HPO_4, 2 mM NaH_2PO_4, and I = 0.15 M NaCl. A stock solution of CT-DNA was prepared and stored in phosphate buffer. The concentration of DNA was determined by UV absorbance at 260 nm using the molar absorption coefficient (6600 M^{-1} CM^{-1}) [28]. The interaction of cationic porphyrins with DNA were determined by

absorption spectro-photometric titrations at a room temperature. Emission spectra of EB bound to DNA in the absence and presence of the TPyPP and TPyPP (Ni) were determined. The induced CD spectra were recorded after the addition of DNA solution to the solution of porphyrin.

2.3. Viscosity measurement

The viscosity of DNA solutions was measured at 30 ± 0.1 °C using an Ubbelohde viscometer. Typically, 10.0 ml of phosphate buffer was transferred to the viscometer to obtain the reading of flow time. For determination of solution viscosity, 10.0 ml of buffered solution of 160 μM DNA was taken to the viscometer and a flow time reading was obtained. An appropriate amount of porphyrin was then added to the viscometer to give a certain r (r = [porphyrin]/[DNA base pair]) value while keeping the DNA concentration constant, and the flow time was read. The flow times of samples were measured after a thermal equilibrium was achieved (30 min). Each point measured was the average of at least five readings. The data obtained were presented as (η/η_0) versus r, where η is the reduced specific viscosity of DNA in the presence of porphyrin and η_0 is the reduced specific viscosity of DNA alone [18,19].

2.4. Electrophoresis test

The compound TPyPP(or TPyPP(Ni) was mixed with plasmid DNA (pBR322) at different molar ratios, after 1.5 h of incubation in the dark at 37 °C. Then electrophoresis experiments were carried out on an electrophoresis system and the gels were stained with EB for 0.5 h after electrophoresis, and then photographed.

3. Results and discussion

3.1. UV–vis spectral studies

The binding of certain complex to DNA produces hypochromism, a broadening of the envelope, and a red shift of the complex absorption band. These effects are particularly pronounced for intercalators, with groove binders, a large wavelength shift usually correlates with a complex conformational change on binding or complex–complex interactions. A spectral change of TPyPP and TPyPP(Ni) with addition of DNA shown in Figs. 1 and 2. They exhibited the hypochromism on the incremental addition of DNA with varying degrees of bathochromic shift, indicating interaction of porphyrin with DNA. The intercalative binding of porphyrin to a DNA helix has been characterized [11] by large changes in the absorbance (hypochromism ≥35%) and an appreciable shift in wavelength (red shift ≥15 nm) due to the interaction of a DNA π stack and porphyrin π system. While outside binders displays smaller red shifts ($\Delta\lambda \leq$ 8 nm) and little hypochromicity ($H \leq 10\%$). The percentage

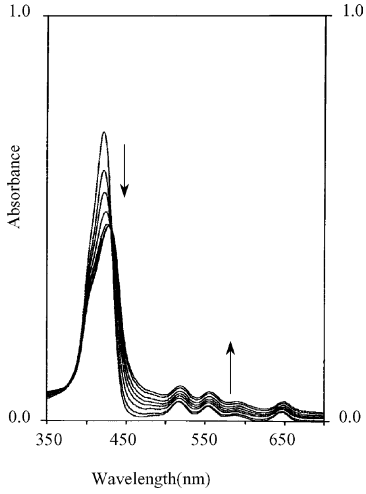

Fig. 1. Absorption spectra of TPyPP (5.8 μM) in the absence (top) and presence of calf thymus-DNA (1.6 μM, 3.2 μM, 4.8 μM, 6.4 μM, 8.0 μM, 9.6 μM, 11.2 μM,) in phosphate buffer pH 7.0 (I = 0.15 M NaCl). Arrow shows that the absorbance changes upon increasing DNA concentration.

hypochromicity of Soret band of TPyPP upon binding to DNA was found to be 32% (hypochromicity, $H\% = \{[(\varepsilon_f - \varepsilon_b)/\varepsilon_f] \times 100\}$, where ε_f and ε_b are the molar absorption coefficients for the free and bound forms of the porphyrin). Red shift was 6.7 nm. The percentage hypochromicity of TPyPP(Ni) with DNA was 35.5%, red shift was 7.4 nm. From above mentioned changes (large hypochromicity and moderate red shift), we considered the interaction TPyPP and its Ni complex with DNA were both out-binding modes.

Binding constants for the interaction of cationic porphyrins with DNA were determined by absorption spectrophotometric titrations at a room temperature. The fixed

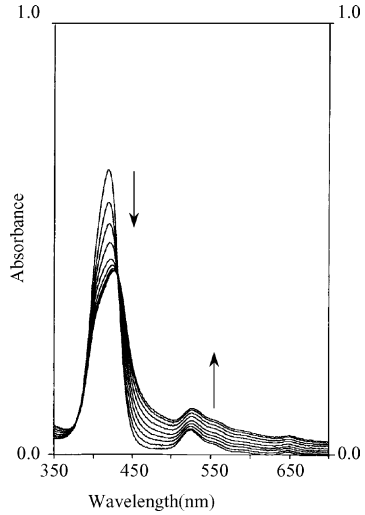

Fig. 2. Absorption spectra of TPyPP(Ni) (5.2 μM) in the absence(top) and presence of DNA (1.6 μM, 3.2 μM, 4.8 μM, 6.4 μM, 8.0 μM, 9.6 μM, 11.2 μM, 12.8 μM) in phosphate buffer pH 7.0 (I = 0.15 M NaCl). Arrow shows that the absorbance changes upon increasing DNA concentration.

amount of cationic porphyrin in phosphate buffer was titrated with a stock solution of DNA. The changes in absorbance of the Soret band upon addition of DNA were monitored at the maximum of the Soret band. The apparent binding constant, K_{app} of cationic porphyrins to DNA was calculated using Eq. (1):

$$\frac{[\mathrm{DNA}]_{total}}{(|\varepsilon_{app} - \varepsilon_f|)} = \left\{\frac{1}{(|\varepsilon_b - \varepsilon_f|)}\right\}[\mathrm{DNA}]_{total} + \frac{1}{\{K_{app}(|\varepsilon_b - \varepsilon_f|)\}} \quad (1)$$

where ε_{app}, ε_f and ε_b correspond to A_{obsd}/[porphyrin], the extinction coefficient for the free porphyrin and the extinction coefficient for the porphyrin in the fully bound form, respectively. In the plot of $[\mathrm{DNA}]_{total}/(|\varepsilon_{app} - \varepsilon_f|)$ versus $\mathrm{DNA}]_{total}$, K_{app} is given by the ratio of the slope to the intercept [29–31]. The apparent binding constants of TPyPP and TPyPP(Ni) were calculated to be $4.65 \times 10^5\ \mathrm{M}^{-1}$and $3.2 \times 10^5\ \mathrm{M}^{-1}$.

The porphyrin TPyPP and TPyPP(Ni) have the flexible tentacles. The flexible tentacle arms of the porphyrin represent a unique characteristic for an outside binder. The tentacles potentially give TPyPP and TPyPP(Ni) a relatively large "footprint" compared to other porphyrins, such that the outside-bound TPyPP and TPyPP(Ni) are able to span several base pairs when bound in either an edge-on or face-on manner [32]. McMillin and co-workers [33] have suggested that outside groove binding produces a larger porphyrin footprint than intercalation.

3.2. Viscosity

Spectroscopic data are necessary, but not sufficient to support a binding mode. As a means for further clarifying the binding of the porphyrins, viscosity measurements were carried out on DNA by varying the concentration of the added porphyrins. A classical intercalative mode causes a significant increase in viscosity of DNA solution due to increase in separation of base pairs at intercalation sites and hence an increase in overall DNA length. By contrast, complexes those bind exclusively in the DNA grooves by partial and/or non-classical intercalation, under the same conditions, typically cause less positive or negative or no change in DNA solution viscosity [34]. Fig. 3 shows the effect of increasing the concentration of porphyrin on the relative viscosity of the DNA. The results reveal that TPyPP and TPyPP(Ni) decreases the relative viscosity of DNA. The decreased relative viscosity of DNA may be explained by an outside-binding mode, which produced bends or kinks in the DNA and thus reduced its effective length and concomitantly its viscosity. The results suggest that non-classical intercalative or out-binding interaction could be ruled out for TPyPP and TPyPP(Ni). We found that the red precipitations were observed visually after time. This phenomenon was observed by Hoffman [35]. Compared TPyPP with TθOPP(meso-tetrakis[4-

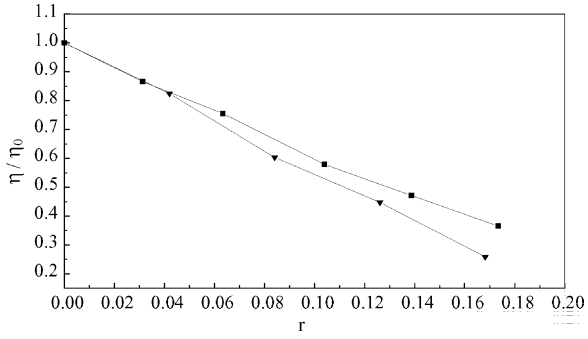

Fig. 3. Effect of increasing amounts of TPyPP (▼),TPyPP(Ni) (■) on the relative viscosities of CT-DNA at 30 ± 0.1 °C and [DNA] = 160 μM and *r* = [porphyrin]/[DNA].

[(3-(trimethylammonio)propyl)-oxy]phenyl] porphine), they have similar structure [12,36]. But Marzilli et al. [36] have not reported TθOPP bind DNA and induce colored precipitate in viscosity measurement. The porphyrins in this investigation have peripherally substituent with N^+ in ring of pyridine, interaction between N^+ and carbon atom in pyridine form a big p–π conjugate system, positive charge distribute the whole pyridine ring, so they have strong ability that attract electron. When they bind negatively charged phosphate oxygen atom which has strong offering electron ability, due to the pyridine small space hindrance, oxygen atom could easily near to nitrogen atom and form a hydrophobic complex whose covalence increase. These measurements show that the long flexible tentacle arms of TPyPP and TPyPP(Ni) probably facilitate favorable outside self-stacking interactions while simultaneously permitting near-optimal electrostatic interaction with the DNA phosphate groups.

3.3. Fluorescence spectroscopic studies

Ethidium bromide (EB) emits intense fluorescence light in the presence of DNA, due to its strong intercalation between the adjacent DNA base pairs. It was previously reported that the enhanced fluorescence can be quenched by the addition of a second molecule [37,38]. The quenching extent of fluorescence of EB bound to DNA is used to determine the extent of binding between the second molecule and DNA. The emission spectra of EB bound to DNA in the absence and the presence of the porphyrins are given in Figs. 4 and 5. According to the classical Stern–Volmer equation [38]:

$$\frac{I_0}{I} = 1 + K_r$$

where I_0 and I are the fluorescence intensities in the absence and the presence of complex, respectively, K a linear Stern–Volmer quenching constant, r the ratio of total concentration of complex to that of DNA. The fluorescence quenching curves of EB bound to DNA by the porphyrins are shown in Figs. 4 and 5. The quenching plots illustrate that the quenching of EB bound to DNA by the porphyrins are

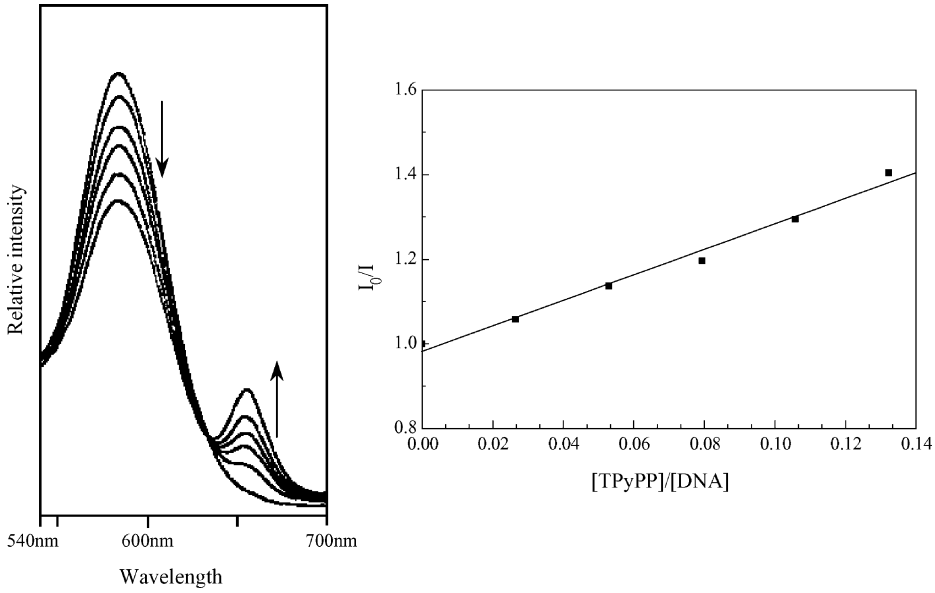

Fig. 4. Emission spectra of EB bound to DNA in the presence of the TPyPP (left), Fluorescence quenching curve of EB bound to DNA by TPyPP (right), [EB] = 5 μM, [DNA] = 12 μM, λ_{ex} = 435 nm. Arrows show the intensity changes upon increasing concentration of the porphyrin, 0, 0.32 μM, 0.64 μM, 0.96 μM, 1.28 μM, 1.5 μM.

in good agreement with the linear Stern–Volmer equation, which also proves that the porphyrins bind to DNA. In the plot of I_0/I versus [porphyrin]/[DNA], K is given by the ratio of the slope to intercept. The K values for TPyPP and TPyPP(Ni) were 3.01 and 2.17, respectively. The data suggests that the interaction of TPyPP with DNA is stronger than TPyPP(Ni), which is consistent with the above absorption spectral results. In the presence of DNA, the excitation spectrum of EB^+ undergoes a large red shift and the excited-state electron becomes easily removable. Many experiments have indicated long-range electron transfer between EB^+ as electron donor or acceptor and drug molecules as electron acceptor or donor, respectively [39,40]. Long-range electron transfer is an important factor, but it is not the only one. Pasternack [41] once suggested the possibility of energy transfer between EB^+ and porphyrins in the presence of DNA. Here the experiments indicate that with increasing concentration of TPyPP, the fluorescence of EB^+ decrease, while the fluorescence of TPyPP appears and increases at 655 nm. The appearance of isoemissive point at 634 nm in the presence of DNA, may indicate complex connection in porphyrin-EB [41]. So interpretation of quenching fluores-

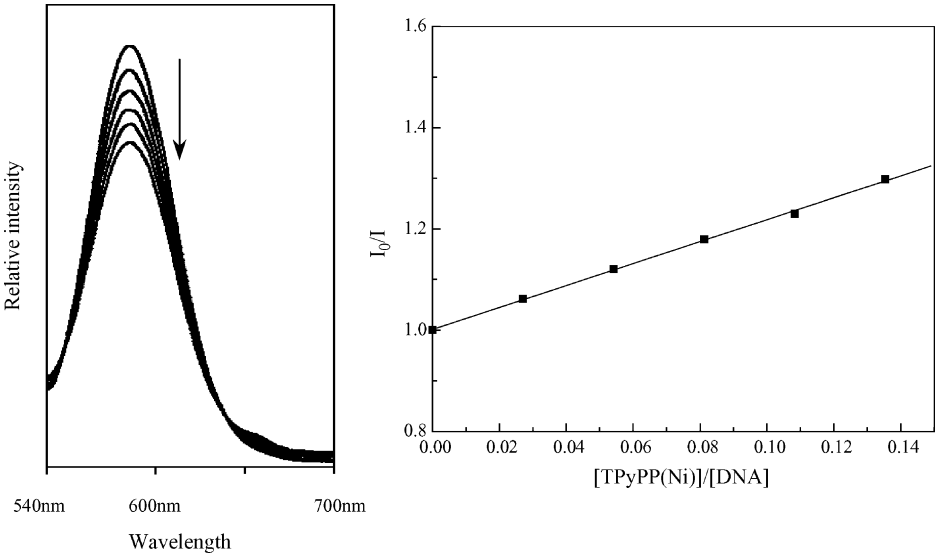

Fig. 5. Emission spectra of EB bound to DNA in the presence of the TPyPP(Ni) (left); Fluorescence quenching curve of EB bound to DNA by TPyPP(Ni) (right), [EB] = 5 μM, [DNA] = 12 μM λ_{ex} = 435 nm. Arrows show the intensity changes upon increasing concentration of the porphyrin 0, 0.32 μM, 0.64 μM, 0.96 μM, 1.28 μM, 1.6 μM.

cence of EB is porphyrin self-stacking along DNA helix and strong interaction electrostatic interactions between the positively charged N substituent on the porphyrin periphery and the negatively charged phosphate oxygen atom of DNA and lead to porphyrin shield EB^+ fluorescence and energy transfer between EB^+ and cationic porphyrin [41].

3.4. Induced CD

In general, DNA binding porphyrins do not possess a chiral center and are optically inactive. However, the CD spectrum in the drug absorption region, especially in the Soret band, is induced when it forms a complex with polynucleotides. Although the origin of induced CD of the achiral porphyrin–DNA complex is not clear, it is believed to be induced by the coupling of the transition moments of achiral drug and chirally arranged nucleobase transition or by excitonic interaction of the DNA-bound drug. The shape and magnitude of induced CD depends on the binding mode and location of the drug, and the nature of the nucleobases [12,42,43]. As shown in Figs. 6 and 7, the TPyPP and TPyPP(Ni) used here do not yield CD spectra in the absence of DNA, but CD spectra were induced for the porphyrins in the presence of DNA, due to the interaction between the transition moments of the achiral porphyrin and chirally arranged DNA base transitions. In Fig. 6, TPyPP displays negative ICD spectra in the 400–430 nm region and positve ICD spectra around 430–460 nm when bound to CT-DNA (r = 0.2), when r = 0.09 the molar ellipiticity ([θ]) both positive([θ] = 1.03 deg dm^2 mol^{-1}) and negative band ([θ] = −1.23 deg dm^2 mol^{-1}) increase slightly. Conservative CD pattern is consistent with an outside binding mode with self-stacking [12,13]. As above studies have shown no increase in DNA solution viscosity upon addition of these two porphyrins. But TPyPP(Ni) display a same behavior as TPyPP, when r = 0.09 a positive band ([θ] = 0.54 deg dm^2 mol^{-1}) at 432 nm, a negative band([θ] = −0.58 deg dm^2 mol^{-1}) at

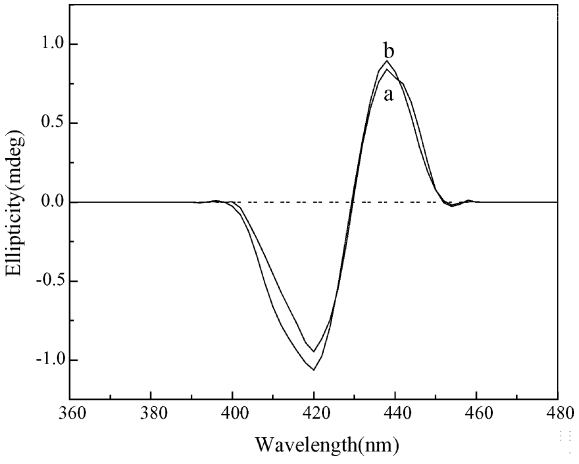

Fig. 6. Induced CD spectra of TPyPP (6.4 μM) in the absence (dashed line) and presence of CT-DNA (solid line) r = 0.2 (a), r = 0.09 (b) in phosphate buffer pH 7.0 (I = 0.15 M NaCl).

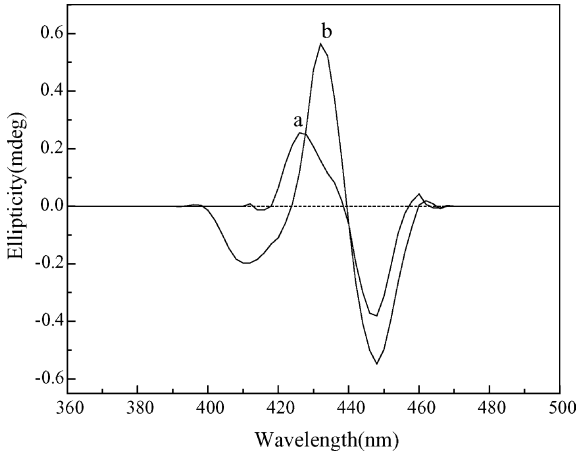

Fig. 7. Induced CD spectra of TPyPP(Ni) 7.8 μM in the absence (dashed line) and presence of CT-DNA (solid line) r = 0.2 (a), r = 0.09 (b) in phosphate buffer pH 7.0 (I = 0.15 M NaCl).

448 nm appear in Fig. 7. When r = 0.2, positive band blue shift to 426 nm ([θ] = 0.3 deg dm^2 mol^{-1}), negative band blue shift slightly to 446 nm ([θ] = −0.44 deg dm^2 mol^{-1}). These results are indicative that TPyPP and its Ni complex bind DNA by out-side self-stacking along the DNA helix, but they self stack by different direction. The porphyrin do not intercalate because of the high electron density in the porphyrin core [33]. These changes in CD spectrum in Soret band reflect binding mode is not obvious varying depend on porphyrins concentration.

3.5. Interaction of porphyrin with plasmid DNA pBR322

Fig. 8 is shown the interaction of porphyrins with pBR322 DNA. Control experiments indicated that no cleavage of DNA happened in the presence porphyrins. But as shown in Fig. 8, with increasing concentration of TPyPP, the lane 1–3 run slower than lane 0 that pBR322 DNA alone. Due to positively charged N substituent on the porphyrin periphery and negatively phosphate oxygen atom of DNA and this interaction is so strong that prevent EB staining. With increasing concentration of TPyPP, the blocking effect is so obvious as to the light of EB in UV lamp disappear (the photo is not shown). While with concentration of TPyPP(Ni) increasing, the lane 4–6 behavior is the same as that of lane 1–3. The rational interpretation is that porphyrin–DNA adduct is tight

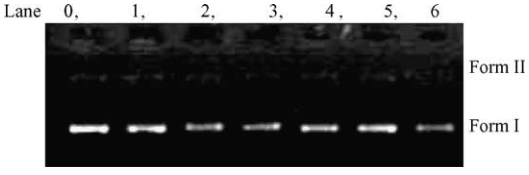

Fig. 8. Interaction of supercoiled pBR322 DNA by porphyrin TPyPP TPyPP(Ni) and 12 μL reaction mixtures contained 40 ng of plasmid DNA. Lane 0: DNA alone; lane 1: DNA + TPyPP (1 μM); lane 2: DNA + TPyPP (5 μM); lane 3: DNA + TPyPP (10 μM); lane 4: DNA + TPyPP(Ni) (1 μM); lane 5:DNA + TPyPP(Ni) (5 μM); lane 6: DNA + TPyPP(Ni) (10 μM).

so that shield EB light. The conclusion is consistent with the front experiment.

4. Conclusion

In the present study, we have synthesized two water-soluble porphyrins and characterized them. Interaction of the porphyrins with DNA is shown here that they can both bind DNA by out-side self-stacking along the DNA helix, but they self stack by different direction. In addition to the porphyrins do not intercalate because of the high electron density in the porphyrin core. The long flexible tentacle arms of porphyrin probably facilitate outside self-stacking interactions while simultaneously permitting near-optimal electrostatic interaction with the DNA phosphate groups.

References

[1] P. Hambright, R. Fawwaz, P. Valk, J. McRac, A.J. Bearden, Bioinorg. Chem. 5 (1975) 87.
[2] G.D. Zanelli, A.C. Kaclin, Br. J. Radiol. 53 (1981) 403.
[3] C. Chen, J.S. Cohen, C.E. Myers, M. Sohn, FEBS Lett. 168 (1984) 70.
[4] N.J. Patronas, M. Cohen, R.H. Knop, A.J. Dwyer, D. Colcher, J. Lundy, F. Mornex, P. Hambright, M. Sohn, C.E. Myers, Cancer Treatment Rep. 70 (1986) 391.
[5] A.M. del, C. Batlle, J. Photochem. Photobiol. 20 (1993) 5.
[6] R. Bonnett, Chem. Soc. Rev. (1995) 19.
[7] I. Ben-Hur, B. Horowitz, Photochem. Photobiol. 62 (1995) 383.
[8] G. Pratviel, J. Bernadou, B. Meunier, Metal Ions in Biological Systems, Marcel Dekker, New York, 1996.
[9] R.M. Burger, Chem. Rev. 98 (1998) 1153.
[10] S. Niedle, M.R. Sanderson, Molecular Aspects of Anti-cancer Drug Action, Verlag Chemie GmBH, Weinheim, 1983.
[11] R.F. Pasternack, E.J. Gibbs, J.J. Villafranca, Biochemistry 22 (1983) 2406.
[12] N.E. Makundan, G. Petho, D.W. Dixon, L.G. Marzilli, Inorg. Chem. 34 (1995) 3677.
[13] R.F. Pasternack, Chirality 15 (2003) 329.
[14] M.A. Sari, J.P. Battioni, D. Dupre, D. Mansuy, J.B. LePecq, Biochemistry 29 (1990) 4205.
[15] K. Butje, J.H. Schneider, J.P. Kim, Y. Wang, S. Ikuta, K. Nakamoto, J. Inorg. Biochem. 37 (1989) 119.
[16] J.A. Strickland, L.G. Marzilli, W.D. Wilson, G. Zon, Inorg. Chem. 28 (1989) 4191.
[17] G. Dougherty, R.F. Pasternack, Biophys. Chem. 44 (1992) 11.
[18] D.L. Banville, L.G. Marzilli, J.A. Strickland, W.D. Wilson, Biopolymers 25 (1986) 1837.
[19] T.A. Gray, K.T. Yue, L.G. Marzilli, J. Inorg. Biochem. 41 (1991) 205.
[20] B. Ward, A. Skorobogaty, J.C. Dabrowiak, Biochemistry 25 (1986) 7827.
[21] K. Ford, K.R. Fox, S. Neidle, M.J. Waring, Nucl. Acids Res. 15 (1987) 2221.
[22] R.F. Pasternack, E.J. Gibbs, J.J. Vilafranca, Biochemistry 22 (1983) 5409.
[23] L.A. Lipscomb, F.X. Zhou, S.R. Presnell, R.J. Woo, M.E. Peek, R.R. Plaskon, L.D. Williams, Biochemistry 35 (1996) 2818.
[24] R.F. Pasternack, E.J. Gibbs, Met. Ions Biol. Syst. 33 (1996) 367.
[25] J.E. McClure, L. Baudouin, D. Mansuy, L.G. Marzilli, Biopolymers 42 (1997) 203.
[26] A.B. Guliaev, N.B. Leontis, Biochemistry 38 (1999) 15425.
[27] R. Lionel, Milgrom, J. Chem. Soc. Perkin Trans. I (1983) 2535.
[28] M.F. Reichmann, S.A. Rice, C.A. Thomas, P. Doty, J. Am. Chem. Soc. 76 (1954) 3047.
[29] A.M. Pyle, J.P. Rehman, R. Meshoyrer, C.V. Kumar, N.J. Turro, J.K. Barton, J. Am. Chem. Soc. 111 (1989) 3051.
[30] J. Onuki, A.V. Ribas, M.H.G. Medeiros, K. Araki, H.E. Toma, L.H. Catalani, P.D. Mascio, Photochem. Photobiol. 63 (1996) 272.
[31] S. Mettath, B.R. Munson, R.K. Pandey, Bioconj. Chem. 10 (1999) 94.
[32] N.E. Mukundan, J.G. PethiiJq, D.W. Dixon, M.S. Kim, L.G. Marzilli, Inorg. Chem. 33 (1994) 4676.
[33] B.P. Hudson, J. Sou, D.J. Berger, D.R. McMillin, J. Am. Chem. Soc. 114 (1992) 8997.
[34] T.M. Kelly, A.B. Tossi, D.J. McConnell, T.C. Strekas, Nucl. Acids Res. 13 (1985) 6017.
[35] M.E. Anderson, A.G.M. Barrett, B.M. Hoffman, J. Inorg. Biochem. 80 (2000) 257.
[36] L.G. Marzilli, T. Gabor Petho, M. Lin, M.S. Kim, D.W. Dixon, J. Am. Chem. Soc. 114 (1992) 7575.
[37] B.C. Baguley, M. LeBret, Biochemistry 23 (1984) 937.
[38] J.R. Lakowicz, G. Webber, Biochemistry 12 (1973) 4161.
[39] P. Fornherz, B. Rieger, J. Am. Chem. Soc. 108 (1986) 5361.
[40] J.K. Barton, C.V. Kumar, N.J. Turro, J. Am. Chem. Soc. 108 (1986) 6391.
[41] R.F. Pasternack, M. Caccam, B. Keogh, J. Am. Chem. Soc. 113 (1991) 6835.
[42] U. Sehlstedt, S.K. Kim, P. Carter, Biochemistry 33 (1994) 417.
[43] B.H. Yun, S.H. Jeon, T.S. Cho, S.Y. Yi, U. Sehlstedt, S.K. Kim, Biophys. Chem. 70 (1998) 1.